Journal of
Materials Chemistry C

Accepted Manuscript

This article can be cited before page numbers have been issued, to do this please use: Y. Lei, Y. Zhou, L. Qian, Y. Wang, M. Liu, X. Huang, G. Wu, H. Wu, J. Ding and Y. Cheng, *J. Mater. Chem. C*, 2017, DOI: 10.1039/C7TC00362E.

ROYAL SOCIETY OF CHEMISTRY

rsc.li/materials-c

View Article Online
DOI: 10.1039/C7TC00362E

Journal of Materials Chemistry C

ARTICLE

Polymorphism and mechanochromism of *N*-alkylated 1,4-dihydropyridine derivatives containing different electron-withdrawing end groups

Received 00th January 20xx,
Accepted 00th January 20xx

DOI: 10.1039/x0xx00000x

www.rsc.org/

Yunxiang Lei,[a] Yibin Zhou,[a] Lebin Qian,[a] Yuxiang Wang,[b] Miaochang Liu,[a] Xiaobo Huang,*[a] Ge Wu,[c] Huayue Wu,*[a] Jinchang Ding[a] and Yixiang Cheng*[b]

Organic compounds exhibiting polymorphic and/or mechanochromic (MC) properties are promising for applications in multiple areas. However, the design strategy for such compounds is not very clear. Herein, several series of N-alkylated 1,4-dihydropyridine (DHP) derivatives incorporating different electron-withdrawing end groups were synthesized and compared. The electron-withdrawing groups were responsible for their polymorphic and MC properties. Additionally, the number of polymorphs of the DHP derivatives showed a decreasing trend as the length of the alkyl chain increased, indicating that a longer alkyl chain was not conducive to the formation of the polymorphs. Although the difference in emissions of polymorphs was mainly attributed to their different intermolecular interactions and molecular packing patterns, a subtle difference in the distances of the intermolecular interactions could also be a key factor in the formation of the specific polymorphs. Different polymorphs of the DHP derivatives could be interconverted by a simple recrystallization process with a specific solvent or through the application of pressure and vapor stimuli. Additionally, the MC properties of these DHP derivatives were ascribed to the phase transition between different crystalline states, not the more common transformation between crystalline and amorphous states.

Introduction

Solid-state organic compounds exhibiting switchable and variable fluorescence have recently attracted considerable interest owing to their potential application in a wide range of fluorescent materials.[1] Two kinds of fluorescence characteristics, namely, mechanochromic (MC) and polymorphic properties, have been of particular interest in the development of these materials. MC compounds are a class of smart fluorescent materials with variable emission in response to pressure stimuli and their fluorescence can often be recovered by the vapor and/or temperature stimuli based on the transformation between crystalline and amorphous states.[1b] Some compounds with polymorphic properties have a variety of crystal structures and exhibit distinctly different solid-state fluorescence,[2] and the interconversion of the emissions of the polymorphs can be ascribed to a transformation from one crystalline state to another crystalline state. Recently, a number of compounds have been found to possess MC and polymorphic properties simultaneously,[3] however, the structural features that influence the presence of both MC and polymorphic properties and the design strategy for such compounds are not very clear, which remains a challenge and deserves further study.

4*H*-Pyran[4] and 1,4-dihydropyridine (DHP)[5] have been demonstrated to be good building units for the construction of donor-π-acceptor fluorescent materials. In particular, the introduction of an alkyl chain on the nitrogen atom is conducive to the formation of a distorted molecular conformation, which results in strong solid-state emission owing to the restriction of the intramolecular rotation.[6] Recently, we reported that some

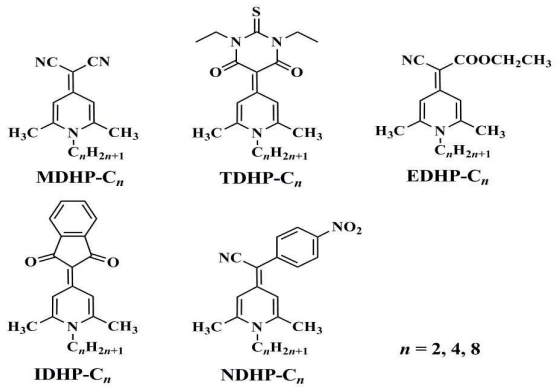

Scheme 1. Chemical structures of DHP derivatives.

[a] College of Chemistry and Materials Engineering, Wenzhou University, Wenzhou, 325035, P. R. China. *E-mail: xiaobhuang@wzu.edu.cn; huayuewu@wzu.edu.cn
[b] School of Chemistry and Chemical Engineering, Nanjing University, Nanjing210093, P. R. China. *E-mail: yxcheng@nju.edu.cn
[c] School of Pharmacy, Wenzhou Medical University, Wenzhou 325035, P. R. China.

† Electronic Supplementary Information (ESI) available: Experimental, characterization, crystal structures (CCDC 1498114-1498127), fluorescence spectra, photophysical data, and other additional information. See DOI: 10.1039/x0xx00000x

View Article Online
DOI: 10.1039/C7TC00362E

aggregation-induced-emission-active 4*H*-pyran and 1,4-dihydropyridine derivatives exhibited MC properties, solvent-induced solid-state emission changes, or acidochromic properties.[7] Unexpectedly, in the course of investigating the photophysical properties of these compounds, we found that an intermediate with a simple structure, 2-(1-ethyl-2,6-dimethylpyridin-4(1*H*)-ylidene)malononitrile (**MDHP-C$_2$**), showed MC and polymorphic properties (Scheme 1). Considering that different electron-withdrawing end groups[7b,8] and alkyl chain lengths[9] often played functional roles in modulating the solid-state photophysical properties, we designed and synthesized several series of DHP derivatives with different alkyl chain lengths (ethyl, *n*-butyl, and *n*-octyl) on the nitrogen atom, namely **MDHP-C$_n$**, **TDHP-C$_n$**, **EDHP-C$_n$**, **IDHP-C$_n$**, and **NDHP-C$_n$** (*n* = 2, 4, 8), using malononitrile, 1,3-diethyl-2-thioxodihydropyrimidine-4,6(1*H*,5*H*)-dione, ethyl 2-cyanoacetate, 1*H*-indene-1,3(2*H*)-dione, and 2-(4-nitrophenyl)acetonitrile as electron-withdrawing end groups, respectively (Scheme 1). The electron-withdrawing end group had a significant impact on the solid-state fluorescence properties of these compounds. Compounds **MDHP-C$_n$**, **TDHP-C$_n$** (except **TDHP-C$_8$**), and **EDHP-C$_n$** all showed polymorphic and MC properties; however, **IDHP-C$_n$** and **NDHP-C$_n$** did not have these properties. Furthermore, the number of polymorphs of **MDHP-C$_n$** and **TDHP-C$_n$** showed a decreasing trend as the length of the alkyl chain increased. The difference in emissions of the polymorphs was mainly attributed to their different intermolecular interactions and molecular packing patterns, but interestingly, a subtle difference in the distances of the intermolecular interactions also played a crucial role in the formation of the polymorphs, as revealed by crystallographic data. Different polymorphs of the DHP derivatives were interconverted by a simple recrystallization process with a specific solvent, grinding, or fuming. Additionally, X-ray diffraction (XRD) and Differential scanning calorimetry (DSC) measurements experiments indicated that the MC properties of these DHP derivatives were ascribed to the phase transition between different crystalline states, not the common transformation between the crystalline and amorphous states.

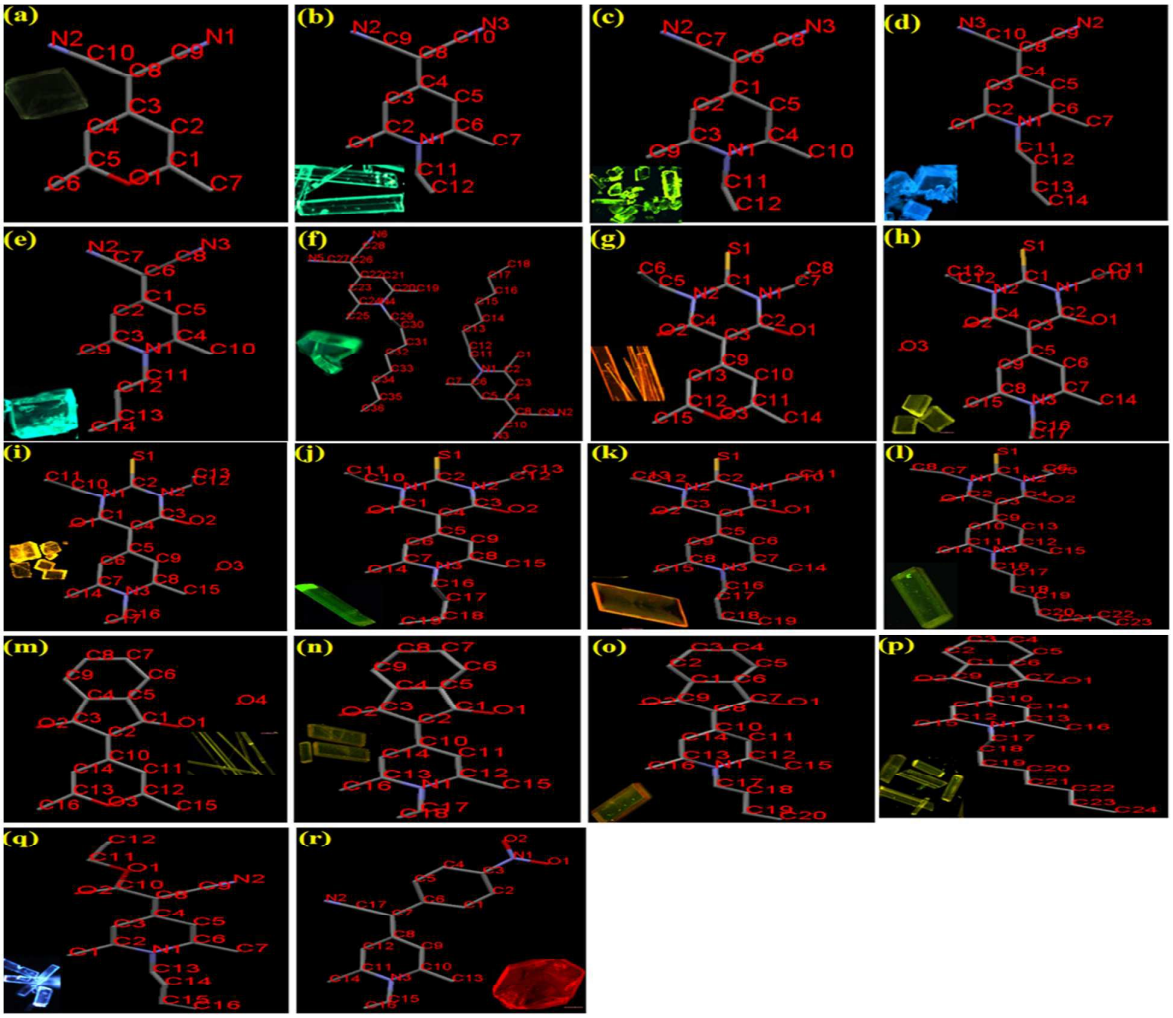

Fig. 1 Single-crystal structures of some 4*H*-pyran and DHP derivatives: (a) **MP**; (b) **MDHP-C$_2$-*c***; (c) **MDHP-C$_2$-*l***; (d) **MDHP-C$_4$-*sb***; (e) **MDHP-C$_4$-*lc***; (f) **MDHP-C$_8$-*c***; (g) **TP**; (h) **TDHP-C$_2$-*ly***; (i) **TDHP-C$_2$-*o***; (j) **TDHP-C$_4$-*g***; (k) **TDHP-C$_4$-*o***; (l) **TDHP-C$_8$**; (m) **IP**; (n) **IDHP-C$_2$**; (o) **IDHP-C$_4$**; (p) **IDHP-C$_8$**; (q) **EDHP-C$_4$**; (r) **NDHP-C$_2$**. Hydrogen atoms are omitted for clarity. Inset: fluorescence image of the corresponding single crystal taken under 365 nm UV light.

View Article Online
DOI: 10.1039/C7TC00362E

Results and discussion

Synthesis and features of 4*H*-pyran and DHP derivatives

The synthetic route of the 4*H*-pyran and DHP derivatives is outlined in Scheme S1†. Compounds **MP**,[6d,10] **MDHP-C$_n$**,[6d,10,11,7d] **EP**,[12] **EDHP-C$_8$**,[12] **IP**,[7a] and **IDHP-C$_n$**[7c] were synthesized according to previous literature procedures. The intermediates **TP** and **NP** were prepared from a Knoevenagel condensation of 2,6-dimethyl-4-pyrone with 1,3-diethyl-2-thioxodihydro- pyrimidine-4,6(1*H*,5*H*)-dione and 2-(4-nitrophenyl)acetonitrile, respectively. The reaction of **TP**, **EP**, and **NP** with the corresponding aliphatic amines gave compounds **TDHP-C$_n$**, **EDHP-C$_2$**, **EDHP-C$_4$**, and **NDHP-C$_n$**, respectively, in good yields. The chemical structures of these compounds were characterized using nuclear magnetic resonance spectroscopy, elementary analysis, and mass spectrometry. Moreover, the structures of **MP**, **MDHP-C$_n$**, **TP**, **TDHP-C$_n$**, **IP**, **IDHP-C$_2$**, **EDHP-C$_4$**, and **NDHP-C$_2$** were further confirmed by single-crystal X-ray diffraction analysis (Fig. 1). The resulting compounds were well soluble in common organic solvents such as tetrahydrofuran, toluene, ethyl acetate (EA), chloroform, acetonitrile, and acetone.

Fluorescence properties of 4*H*-pyran and DHP derivatives solids

The fluorescence spectra, excitation spectra, and fluorescence quantum yields (Φ_F) of the as-synthesized solids of various 4*H*-pyran derivatives were measured (Fig. S1, Table S1, and Table S2, ESI†). The electron-withdrawing end groups had a significant impact on the solid-state fluorescence spectra of the 4*H*-pyran derivatives. Among the compounds, **MP** and **NP** showed the smallest and largest maximum emission wavelength (λ_{em}^{max}) at 481 and 599 nm with a low Φ_F value of 0.6 and 2.0%, respectively. The Φ_F values of **TP**, **EP**, and **IP** were 2.0, 31.4, and 20.4%, respectively. For the sake of discussion, herein, the solids of all the DHP derivatives obtained by a recrystallization of their as-synthesized solids using a mixed solvent of *n*-hexane and $CHCl_3$ (30:1, v:v) were regarded as their original samples. The fluorescence spectra of the original samples of **MDHP-C$_n$**, **TDHP-C$_n$**, and **EDHP-C$_n$** showed an obvious blueshift compared with those of the corresponding 4*H*-pyran derivatives, whereas the original samples of **IDHP-C$_n$** and **NDHP-C$_n$** exhibited an obvious redshift (Fig. S2, ESI†). Although the introduction of an *N*-alkyl chain is beneficial for the enhancement of degree of distortion of the molecular structure and the promotion of a blueshift in the fluorescence spectra,[7c] the emissions of the solid materials are also closely related to the molecular packing patterns.

Polymorphic and MC properties of DHP derivatives

The synthetic route of the 4*H*-pyran and DHP derivatives is outlinedThe original sample of **MDHP-C$_2$** emitted strong blue fluorescence at 461 nm with a Φ_F value of 48.8% (Fig. 2, Fig. 3, and Table S1, ESI†). Moreover, two different types of single-crystal structures of **MDHP-C$_2$**, namely **MDHP-C$_2$-*c*** and **MDHP-C$_2$-*l***, were cultured by slow diffusion of *n*-hexane into the $CHCl_3$ solution of the original sample and recrystallization using acetonitrile as a solvent, respectively. **MDHP-C$_2$-*c*** emitted cyan fluorescence at 470 nm with a Φ_F value of 79.7%, whereas, lawngreen-emitting **MDHP-C$_2$-*l*** exhibited a redder emission at 489 nm with a lower quantum yield of 57.2%. According to the XRD measurements, the diffraction

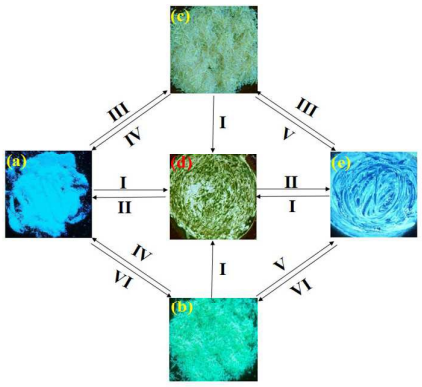

Fig. 2 Fluorescence images of **MDHP-C$_2$** solid samples taken under UV irradiation at 365 nm: (a) original sample; (b) **MDHP-C$_2$-*c*** sample; (c) **MDHP-C$_2$-*l*** sample; (d) Strongly ground sample; (e) Gently ground sample. Conditions: (I) hard grinding; (II) fuming with EA vapor; (III) a recrystallization process using acetonitrile as a solvent; (IV) a recrystallization process using *n*-hexane/$CHCl_3$ (30:1, v:v); (V) gentle grinding; (VI) slow diffusion of *n*-hexane/$CHCl_3$ (6:1, v:v).

curves of the original sample, **MDHP-C$_2$-*c***, and **MDHP-C$_2$-*l*** all revealed sharp and intense reflection peaks (Fig. 4), which were characteristic properties of microcrystalline structures. The results suggested that **MDHP-C$_2$** should be a polycrystalline fluorophore. The difference in emissions between different crystal structures could be mainly attributed to the different intermolecular interactions and molecular packing patterns,[2d] which would be discussed in the crystal structure analysis section below. The three crystal polymorphs could be interconverted by a simple recrystallization process with an appropriate solvent (Fig. 2). A fluorescence color change from blue to yellow-green ($\Delta\lambda_{MC}$ = 41 nm, Table S1, ESI†) was clearly observed after the original crystalline sample of **MDHP-C$_2$** was ground with a pestle in a mortar, suggesting that the original sample exhibited distinct MC properties. If the ground sample was exposed to EA vapor, the fluorescence returned to that of the original sample, suggesting a reversible MC behavior. It was noteworthy that the reflection peaks in the XRD curve of the ground sample were still sharp and intense except that several peaks (2θ = 17.4°, 24.3°, and 26.9°) showed

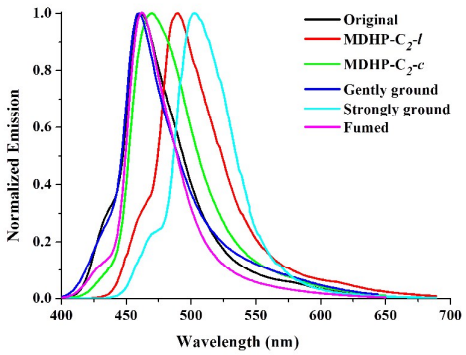

Fig. 3 Normalized emission spectra of **MDHP-C$_2$** solid samples under different conditions.

View Article Online
DOI: 10.1039/C7TC00362E

obvious changes (Fig. 4), indicating the ground sample should also have a crystalline structure. Furthermore, according to the DSC experiments, no cold-crystallization transition was detected before the isotropic melt transition of the ground sample (Fig. S3, ESI†), indicating that the ground sample should not be amorphous but crystalline. The results indicated that the MC properties could be ascribed to the phase transition between different crystalline states,[2h,3d] not the common transformation between crystalline and amorphous states. Moreover, we investigated the stimulus response behavior of **MDHP-C$_2$-*c*** and **MDHP-C$_2$-*l*** upon grinding. Interestingly, by grinding these two types of single crystals with a gentle pressure, blue-emitting solid (λ_{em} = 459 nm, Φ_F = 51.3%) in line with the original sample was obtained, whereas yellow-green-emitting solid (λ_{em} = 502 nm, Φ_F = 40.3%) was obtained using a hard pressure, same as the ground sample obtained from the original sample, indicating **MDHP-C$_2$-*c*** and **MDHP-C$_2$-*l*** displayed multicolored MC behavior. The results demonstrated that the emissions of **MDHP-C$_2$** could be switched between four colors in the solid state by the transformation between four crystalline forms.

MDHP-C$_4$ had three different crystal polymorphs (Fig. 5, Fig. S4, Fig. S5, and Table S1, ESI†), including the original sample (λ_{ex}^{max} = 447 nm, Φ_F = 30.1%), **MDHP-C$_4$-*sb*** (λ_{ex}^{max} = 456 nm, Φ_F = 38.9%), and **MDHP-C$_4$-*lc*** (λ_{ex}^{max} = 466 nm, Φ_F = 18.1%). Upon slow diffusion of *n*-hexane/$CHCl_3$ (6:1, v:v), single crystals of **MDHP-C$_4$-*sb*** with sky-blue emission were formed, whereas single crystals of **MDHP-C$_4$-*lc*** with light cyan emission were obtained by a recrystallization with acetonitrile (Fig. 5). In contrast to **MDHP-C$_2$**, after being ground, the original blue-emitting sample of **MDHP-C$_4$** did not show an obvious fluorescence color change, whereas **MDHP-C$_4$-*sb*** and **MDHP-C$_4$-*lc*** displayed a blueshift of 9 and 19 nm and returned to the original crystal sample (Fig. S3, ESI†), respectively, exhibiting MC properties. In comparison to **MDHP-C$_2$** and **MDHP-C$_4$**, only two types of crystals for **MDHP-C$_8$**, namely the original sample and cyan-emitting **MDHP-C$_8$-*c*** were obtained (Figs. S6-S8, ESI†), indicating a longer alkyl chain was unfavorable for the formation of polymorphic crystals. Moreover, the grinding of **MDHP-C$_8$-*c*** altered its emission from cyan to blue and the ground sample was almost identical to the original sample.

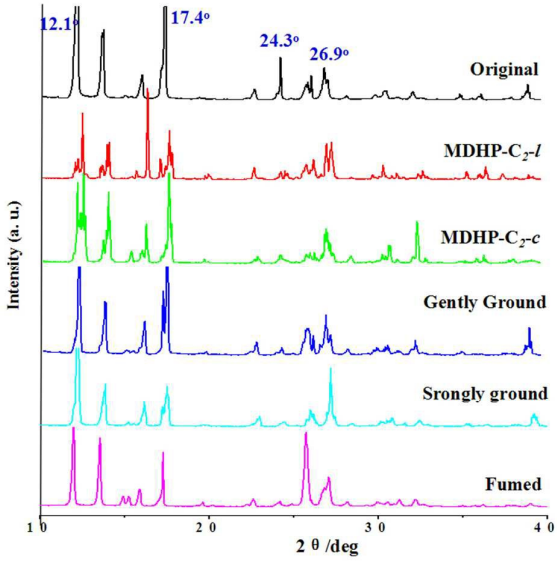

Fig. 4 XRD curves of **MDHP-C$_2$** solid samples under different conditions. The peaks of the original sample at 2θ = 12.1° and 17.4° are truncated for better showing the fine structure.

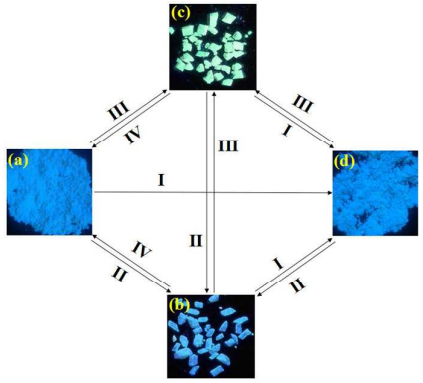

Fig. 5 Fluorescence images of **MDHP-C$_4$** solid samples taken under UV irradiation at 365 nm: (a) original sample; (b) **MDHP-C$_4$-*sb*** sample; (c) **MDHP-C$_4$-*lc*** sample; (d) ground sample. Conditions: (I) grinding; (II) slow diffusion of *n*-hexane/$CHCl_3$ (6:1, v:v); (III) a recrystallization process using CH_3CN as a solvent; (IV) a recrystallization process using a *n*-hexane/$CHCl_3$ (30:1, v:v).

Similarly, **TDHP-C$_2$** and **TDHP-C$_4$** also exhibited polymorphic and MC properties, and showed three and five individual emission colors in the crystalline state, respectively. The original crystalline sample of **TDHP-C$_2$** exhibited weak pale-yellow fluorescence with a Φ_F value of 7.5% (Fig. 6 and Table S1, ESI†). The two crystalline polymorphs **TDHP-C$_2$-*ly*** and **TDHP-C$_2$-*o*** obtained from a slow diffusion of *n*-hexane/$CHCl_3$ (6:1, v:v) and a slow evaporation of $CHCl_3$/EA (1:6, v:v) displayed light yellow (λ_{em} = 458, 596 nm) and orange (λ_{em} = 456, 597 nm) fluorescence, respectively, with quantum yields of 12.2% and 10.7%. After grinding, the ground samples of these two crystals exhibited a similar XRD curve and fluorescence spectrum as those of the original sample (Fig. S9 and

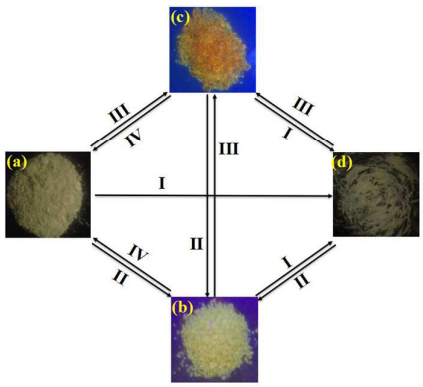

Fig. 6 Fluorescence images of **TDHP-C$_2$** solid samples taken under UV irradiation at 365 nm: (a) original sample; (b) **TDHP-C$_2$-*ly***; (c) **TDHP-C$_2$-*o***; (d) ground sample. Conditions: (I) grinding; (II) slow diffusion of *n*-hexane/$CHCl_3$ (6:1, v:v); (III) slow evaporation of $CHCl_3$/EA (1:6, v:v); (IV) a recrystallization process using a *n*-hexane/$CHCl_3$ (30:1, v:v).

View Article Online
DOI: 10.1039/C7TC00362E

Fig. S10, ESI†). For **TDHP-C$_4$** (Fig. 7, Fig. S11, and Fig. S12, ESI†), interestingly, two kinds of original samples, namely yellow-emitting solids **TDHP-C$_4$-OSA** (λ_{em} = 463, 542 nm, Φ_F = 14.7%) and darkseagreen-emitting solids **TDHP-C$_4$-OSB** (λ_{em} = 456, 533 nm, Φ_F = 10.9%) were obtained by recrystallization using *n*-hexane/$CHCl_3$ with a different volume ratio (v:v = 30:1 for the former and v:v = 60:1 for the latter). There was a slow precipitation process for the former and a fast precipitation process for the latter, indicating that different recrystallization methods led to different morphologies.[3e] Furthermore, green-emitting single crystal **TDHP-C$_4$-*g*** (λ_{em} = 508 nm, Φ_F = 15.9%) was generated by slow diffusion of *n*-hexane/$CHCl_3$ (6:1, v:v) and another orange-emitting single crystal **TDHP-C$_4$-*o*** (λ_{em} = 543, 581 nm, Φ_F = 20.1%) was obtained by slow evaporation of $CHCl_3$/EA (1:6, v:v). After grinding, the two original samples and the two crystalline polymorphs all converted to the solids with yellow-green emission (λ_{em} = 467, 538 nm, Φ_F = 11.2%). For **TDHP-C$_8$**, only a green-emitting crystal sample was obtained, and the fluorescent color and XRD curves did not show a clear change after grinding, suggesting it was MC inactive (Fig. S13, and Fig. S14, ESI†). Generally, **TDHP-C$_2$-*ly***, **TDHP-C$_4$-*g***, and **TDHP-C$_4$-OSB**, which exhibit blue-shifted emissions, should have higher fluorescence efficiencies than **TDHP-C$_2$-*o***, **TDHP-C$_4$-*o***, and **TDHP-C$_4$-OSA**, which exhibit red-shifted emissions, owing to the stronger intermolecular interaction (see below); however, the opposite results were observed (Table S1, ESI†). To explain this abnormal phenomenon, we investigated the time-resolved fluorescence decay parameters of these TDHP derivatives in the solid state (Table S3, ESI†). As shown in Table S3 (ESI†), compared with **TDHP-C$_2$-*o*** and **TDHP-C$_4$-OSA**, **TDHP-C$_2$-*ly*** and **TDHP-C$_4$-OSB** had a smaller radiative rate constant (k_f) and a larger non-radiative rate constant (k_{nr}), respectively. Additionally, although the k_f value of **TDHP-C$_4$-*g*** was 5.4×10^7 s^{-1} and larger than that of **TDHP-C$_4$-*o*** (3.7×10^7 s^{-1}), the k_{nr} value (2.9×10^8 s^{-1}) of **TDHP-C$_4$-*g*** was nearly two times higher than that of **TDHP-C$_4$-*o*** (1.5×10^8 s^{-1}). Herein, the larger non-radiative decay results in fluorescence quenching, which might account for the lower fluorescence efficiencies of the TDHP derivatives with bluer emissions.[3d]

After grinding, changes in the fluorescence color of the original samples of **EDHP-C$_n$** were clearly observed (Fig. S15, ESI†). Interestingly, although there was only a 4 and 5 nm redshift in the maximum emission wavelengths for the original samples of **EDHP-C$_2$** and **EDHP-C$_4$**, respectively, after they were ground (Fig. S16 and Table S2, ESI†), their emission profiles displayed obvious changes, namely, the intensity of the peak at approximately 424 nm showed a remarkable decrease, which could explain the changes in the fluorescence color. Although grinding led to changes to some reflection peaks in the XRD curves of **EDHP-C$_n$** solids (Fig. S17, ESI†), their crystalline structures were still maintained. Meanwhile, there was no cold-crystallization phenomenon observed upon heating the ground samples according to the DSC curves (Fig. S18, ESI†). These results indicated that **EDHP-C$_n$** solids have two kinds of crystal polymorphs and their MC properties were caused by a crystal-to-crystal transformation. After the ground samples were fumed with EA vapor, the emission colors and fluorescent spectra were reversed to those of the emissive original samples. For yellow-emitting **IDHP-C$_n$** (Figs. S19-S21, ESI†) and red-emitting **NDHP-C$_n$** (Figs. S22-S24, ESI†), only one kind of crystal form was obtained and grinding had no obvious influence on the fluorescence spectra and XRD curves of their solid samples, and thus could not change the fluorescence colors. Especially, solid-state **NDHP-C$_4$** did not emit fluorescence but the reason remained unclear because its single crystal could not be obtained.

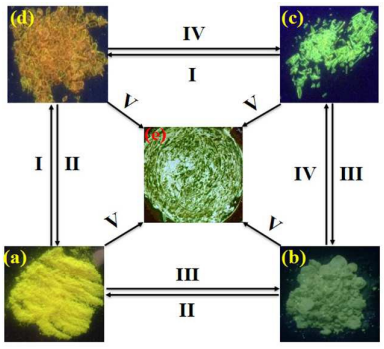

Fig. 7 Fluorescence images of **TDHP-C$_4$** solid samples taken under UV irradiation at 365 nm: (a) **TDHP-C$_4$-OSA**; (b) **TDHP-C$_4$-OSB**; (c) **TDHP-C$_4$-*g***; (d) **TDHP-C$_4$-*o***; (e) ground sample. Conditions: (I) slow evaporation of $CHCl_3$/EA (1:6, v:v); (II) a recrystallization process using *n*-hexane/$CHCl_3$ (30:1, v:v); (III) a recrystallization process using *n*-hexane/$CHCl_3$ (60:1, v:v); (IV) slow diffusion of *n*-hexane/$CHCl_3$ (6:1, v:v); (V) grinding with a pestle in a mortar.

Crystal Structures of DHP derivatives

To gain a better understanding of the underlying reason for the photophysical behaviors of the DHP derivatives in different aggregated states, crystal structure analysis was performed to investigate their molecular conformation and packing pattern in the crystalline state. For the two crystal polymorphs of **MDHP-C$_2$**, the unit cells of **MDHP-C$_2$-*c*** and **MDHP-C$_2$-*l*** were both triclinic with a $P\bar{1}$ space group (Table S4, ESI†). In contrast to that of **MP**, which had a planar structure, these two polymorphs adopted a twisted conformation in which the torsion angles between the *N*-ethyl group and the DHP unit were 80.23° and 80.01°, respectively. The molecules of the crystals of **MDHP-C$_2$-*c*** were stabilized by π–π stacking interactions and C–H···N bonds (Fig. 8). The distances between the DHP unit and the olefinic double bond in the upper and lower molecules were measured to be 3.625 and 3.412 Å, respectively, indicating the existence of π-π stacking. Furthermore, two types of aliphatic C–H···N bonds (2.677 and 2.653 Å) between the H atom of the ethyl moiety and the N atom in the cyano group were formed in the same column, and another C–H···N bond (2.714 Å) restricted the adjacent molecules between the two columns. There were no π-π stacking in the crystal of **MDHP-C$_2$-*l*** and only three kinds of aliphatic C–H···N bonds (2.707, 2.739, and 2.742 Å) restricted the adjacent molecules. The results indicated that crystal of **MDHP-C$_2$-*c*** had stronger intermolecular interactions than the crystal of **MDHP-C$_2$-*l***. We further investigated the molecular packing modes of **MDHP-C$_2$-*c*** and **MDHP-C$_2$-*l*** in the crystals. As shown in Fig. 9, although these two crystal polymorphs both adopted a head-to-tail packing pattern, their packing arrangements showed distinct differences. The molecules of **MDHP-C$_2$-*l*** and **MDHP-C$_2$-*c*** along the *b*-axis were arranged in a single chain and ribbons, respectively. Furthermore, for **MDHP-C$_2$-*l***, the overlap between two pairs of head-to-tail molecules along *c*-axis was obviously poorer compared

View Article Online
DOI: 10.1039/C7TC00362E

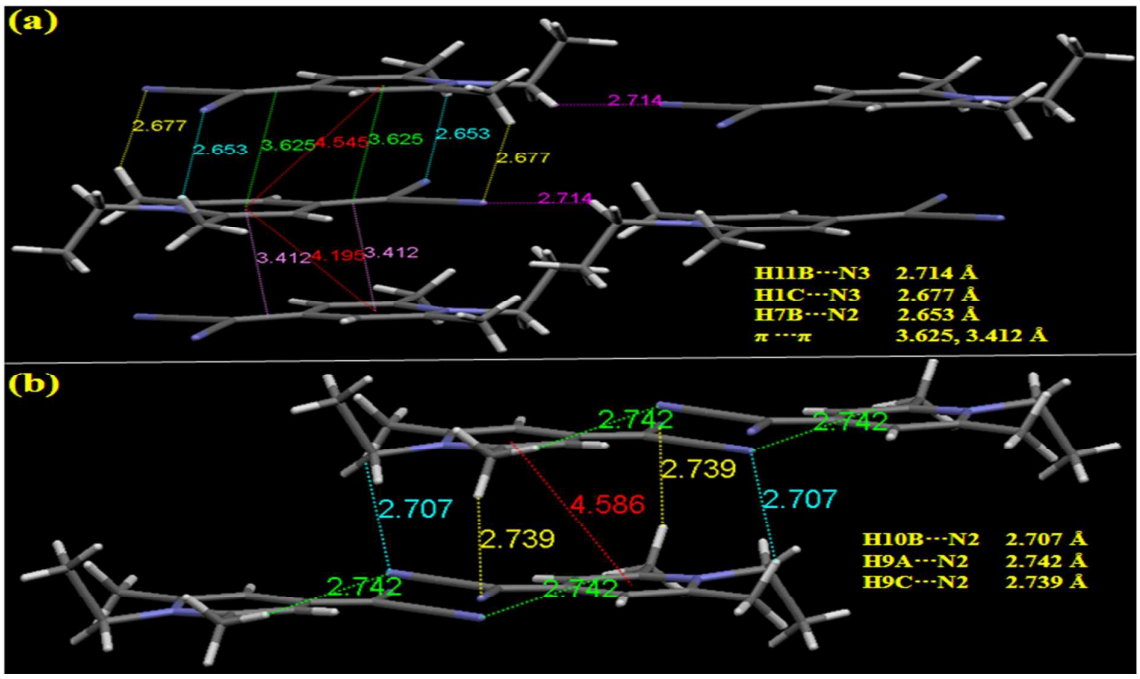

Fig. 8 Schematic diagram of the intermolecular interactions in the crystals of **MDHP-C_2-*c*** (a) and **MDHP-C_2-*l*** (b).

with that of **MDHP-C_2-*c***. The results indicated that the packing of **MDHP-C_2-*c*** in the crystal were more compact compared to those of **MDHP-C_2-*l***. Stronger intermolecular interactions and close molecular packing should inhibit the molecules of **MDHP-C_2-*c*** to have some sort of motion and thus lead to blueshifted emission and higher Φ_F value compared to those of **MDHP-C_2-*l***.[3j] The results also indicated that the different intermolecular interactions and molecular packing arrangements were the main reasons for the observed polymorphism of **MDHP-C_2**. Because of the parallel stacking patterns in these two crystals, it was relatively easy for the crystal structure to change into other crystal forms upon gentle or hard grinding, and thus resulting in MC properties. However, their crystalline structures were not easy to be destroyed by grinding because of strong intermolecular interactions. Therefore, the MC properties could be ascribed to the transformation between different crystalline states. Although the original/gently ground sample emitting blue fluorescence was obtained by recrystallization using a mixed solvent of *n*-hexane and $CHCl_3$, unfortunately, only the single crystal of cyan-emitting **MDHP-C_2-*c***, not that of the original/gently ground sample, was obtained by slow diffusion of *n*-hexane/$CHCl_3$, even using a variety of different volume ratio. Therefore, we were unable to investigate the transformation between different crystalline states.

In the case of the crystal polymorphs of **TDHP-C_2**, the unit cell of **TDHP-C_2-*ly*** was monoclinic with a *P*2(1)/*n* space group and that of **TDHP-C_2-*o*** was monoclinic with a *P*2(1)/*n* space group (Table S5, ESI†). **TDHP-C_2-*ly*** and **TDHP-C_2-*o*** both adopted a head-to-tail packing pattern in pairs, in which the DHP ring stacked with the 2-thioxodihydropyrimidine ring in a face-to-face manner, and the

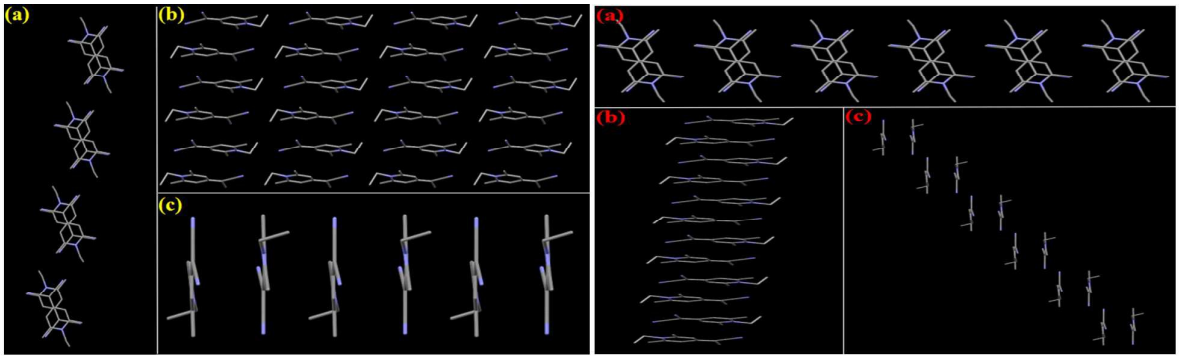

Fig. 9 Packing patterns in the crystal of **MDHP-C_2-*c*** (left) and **MDHP-C_2-*l*** (right): (a) viewed along the *a*-axis; (b) viewed along the *b*-axis; (c) viewed along the *c*-axis. The hydrogen atoms have been omitted for clarity.

View Article Online
DOI: 10.1039/C7TC00362E

dihedral angle between two pairs of molecules was 85.18° and 85.29°, respectively. These two crystal polymorphs were stabilized by weak π–π stacking interactions (3.849 Å for **TDHP-C_2-*ly*** and 3.857 Å for **TDHP-C_2-*o***), aliphatic C–H···S bonds (2.975 Å for **TDHP-C_2-*ly*** and 2.984 Å for **TDHP-C_2-*o***), and aliphatic C–H···π bonds (3.275–3.698 Å for **TDHP-C_2-*ly*** and 3.281–3.756 Å for **TDHP-C_2-*o***) from adjacent molecules, whereas, the interaction distances of **TDHP-C_2-*ly*** were obviously shorter than those of **TDHP-C_2-*o*** (Fig. 10). Moreover, as depicted in Fig. 11, although they exhibited the same packing arrangement along the *a*-axis, the packing of **TDHP-C_2-*o*** along the *b*-axis and the *c*-axis was looser compared with that of **TDHP-C_2-*ly***, which should be the reason that the emission of the former showed obvious red shift compared to that of the latter.

The crystals of **MDHP-C_4-*sb*** and **MDHP-C_4-*lc*** were mainly stabilized by C–H···N bonds, C–H···π bonds, and π–π stacking interactions between the DHP rings (Fig. S25, ESI†). Interestingly, these two polymorphs showed the same molecular packing pattern in the crystals (Fig. S26, ESI†). There was a subtle difference in the distances of the intermolecular interactions of **MDHP-C_4-*sb***, which were all shorter than the corresponding distances of **MDHP-C_4-*lc*** (Fig. S25, ESI†), indicating more intense intermolecular forces between the molecules in the former crystals. As a result, the molecules in the crystal lattice of **MDHP-C_4-*sb*** accumulated more

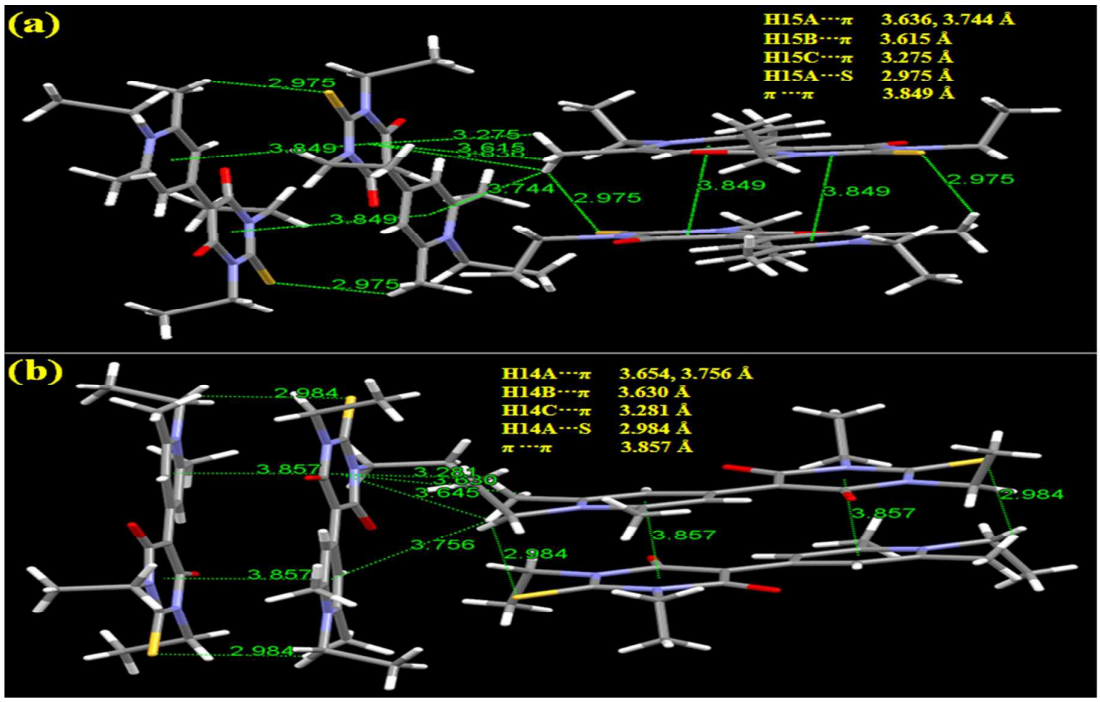

Fig. 10 Schematic diagram of the intermolecular interactions in the crystals of **TDHP-C_2-*ly*** (a) and **TDHP-C_2-*o*** (b).

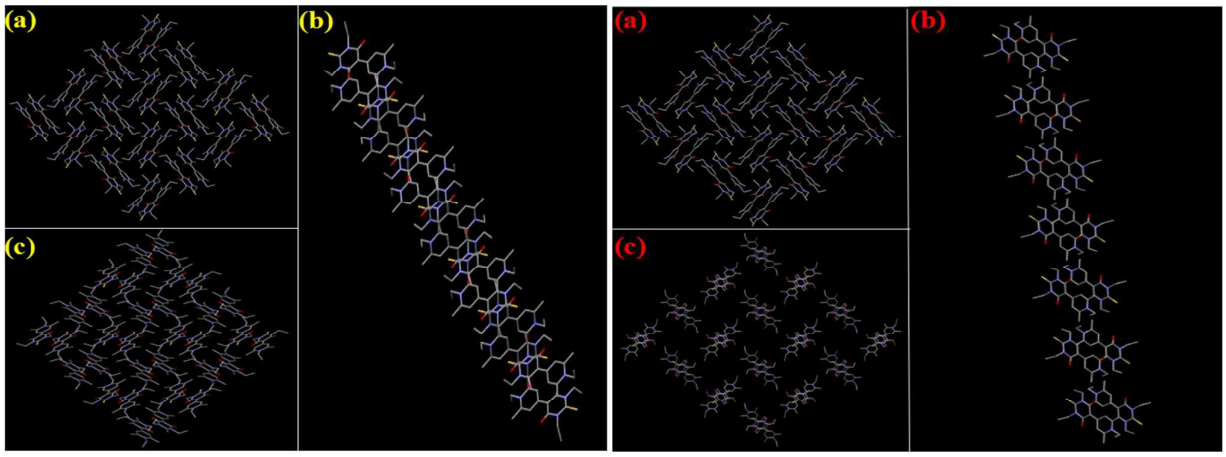

Fig. 11 Packing patterns in the crystal of **TDHP-C_2-*ly*** (left) and **TDHP-C_2-*o*** (right): (a) viewed along the *a*-axis; (b) viewed along the *b*-axis; (c) viewed along the *c*-axis. The hydrogen atoms have been omitted for clarity.

View Article Online
DOI: 10.1039/C7TC00362E

closely and thus had a smaller volume and a bigger density (655.05 Å^3 and 1.152 Mg/m^3) compared to those of **MDHP-C$_4$-*lc*** (680.9 Å^3 and 1.109 Mg/m^3) (Table S4, ESI†). A similar phenomenon was observed in the two polymorphs of **TDHP-C$_4$**, namely **TDHP-C$_4$-*g*** and **TDHP-C$_4$-*o***, (Fig. S27, Fig S28 and Table S4, ESI†). Based on the results, a minor difference in the distances of the intermolecular interactions can also play a crucial role in the formation of the polymorphs.

It should be noted that the number of polymorphs of **TDHP-C$_n$** and **MDHP-C$_n$** generally decreased as the length of the alkyl chain increased. Only two types of crystals were obtained for **MDHP-C$_8$** and one type for **TDHP-C$_8$**. **MDHP-C$_8$-*c*** belonged to the monoclinic crystal system and had a *Pc* space group (Table S4, ESI†). There were six kinds of intermolecular C–H···N bonds (2.516–2.735 Å) and five kinds of C–H···π bonds (2.840–3.494 Å) in the crystal (Fig. S29, ESI†). Compared with the polymorphs of **MDHP-C$_2$** and **MDHP-C$_4$**, the regularity and rigidity of the crystal alignment of **MDHP-C$_8$-*c*** was clearly poorer as a result of the introduction of long *n*-octyl chain, indicating that the *n*-octyl group was not advantageous to the varied balance of the weak intermolecular interactions between molecules in the solid state and thereby the formation of different polymorph. Additionally, **MDHP-C$_8$-*c*** had a bigger volume (1664.7 Å^3) and a smaller density (1.131 Mg/m^3) in the crystal lattice (Table S5, ESI†). For **TDHP-C$_8$**, two kinds of C–H···O bonds (2.519 and 2.520 Å) and four kinds of π···π interactions (3.351–3.723 Å) stabilized the crystal structure (Fig. S30, ESI†). Interestingly, **TDHP-C$_8$**, which was quite different from the other **MDHP** and **TDHP** derivatives, did not show MC properties, which might be attributed to its one kind of crystal form and thus the transformation from a crystalline state to another crystalline state could not be implemented.

As for **EDHP-C$_n$**, we just only obtained the blue-emitting single crystal of **EDHP-C$_4$** from a slow diffusion of *n*-hexane/$CHCl_3$ (6:1, v:v). As revealed by the crystal structure of **EDHP-*C*$_4$** (Fig. S31, ESI†), the molecules in the same layer were restricted by one kind of aliphatic C–H···O bond (2.336 Å), and those in the upper and lower layers were stabilized by one kind of π–π stacking interaction (3.513 Å), one kind of aliphatic C–H···O bond (2.669 Å), and one kind of van der Waals force between aliphatic hydrogen atoms in the *N*-butyl chains (with a distance of 2.383 Å). As a result, the molecules of **EDHP-C$_4$** adopted a stairs-like stacking mode, which allowed it to be easily changed into another crystal mode upon grinding.

In the case of **IDHP-C$_n$**, the yellow-emitting single crystal of **IDHP-C$_2$** was obtained from slow diffusion of *n*-hexane/$CHCl_3$ (6:1, v:v), and the crystal data of **IDHP-C$_4$** and **IDHP-C$_8$** was obtained from our previous report.[7c] The molecules of **IDHP-C$_2$**, **IDHP-C$_4$**, and **IDHP-C$_8$** in the crystal were stabilized by one kind of π–π stacking interaction, two kinds of C–H···π bonds, and two, six, and four kinds of C–H···O bonds between adjacent molecules, respectively (Figs. S32-S34, ESI†). **IDHP-C$_2$** and **IDHP-C$_4$** both adopted a head-to-tail packing pattern in pairs and packed in a tight zigzag shape. Herein, because of the strong intermolecular interactions and tight packing mode, the crystal structures of these compounds were not easy to change upon grinding, which was also confirmed by the results from the XRD experiments before and after grinding (Fig. S21, ESI†). Although **IDHP-C$_8$** packed in a reverse lamellar structure, strong intermolecular interactions still guaranteed the stability of the crystal structure, avoiding being affected by external pressure (Fig. S34, ESI†).

The unit cell of **NDHP-C$_2$** was monoclinic with a *P*2(1)/*c* space group (Table S6, ESI†). As revealed by the crystal structure of **NDHP-C$_2$** (Fig. S35, ESI†), the molecule exhibited a twisted conformation due to the introduction of steric hindrance from a big 4-nitrophenyl group, and the dihedral angle between the DHP ring and the benzene ring was 35.29°. Interestingly, in comparison with the other DHP derivatives containing an *N*-ethyl group, the original sample of **NDHP-C$_2$** had a bigger emission wavelength (640 nm) and emitted red fluorescence, which was ascribed to the stronger electron withdrawing ability and larger conjugated system of the 4-nitrophenyl group. The distance between the two phenyl rings in the upper and lower layers was measured to be 4.066 Å, which indicated the absence of π-π stacking. The crystal structure was stabilized by three kinds of C–H···N bonds (2.689, 2.703, and 2.705 Å), two kinds of C–H···π bonds (2.793 and 2.811 Å), and one kind of C–H···O bond (2.935 Å) from adjacent molecules, adopting an offset face-to-face arrangement in the upper and lower layers and a head-to-tail arrangement in the same layer. Similar to **IDHP-C$_8$**, strong interactions between molecules ensured that the crystal structure of this compound was not damaged by grinding.

Conclusions

Several series of DHP derivatives were synthesized to investigate the influence of different electron-withdrawing end groups and alkyl chain lengths on their possible polymorphic and MC properties. Most of **MDHP-C$_n$**, **TDHP-C$_n$**, and **EDHP-C$_n$** had a variety of crystals emitting different fluorescence and showed obvious MC properties; however, compounds **IDHP-C$_n$** and **NDHP-C$_n$** only have one type of crystal and were MC inactive. The results revealed that the electron-withdrawing end group played a vital role in the generation of MC and polymorphic properties of the DHP derivatives. The possible reason was that the electron-withdrawing end group with different steric and electronic effect had a significant influence on the generation of appropriate intermolecular interactions between molecules and proper molecular packing patterns in the crystals which could result in the formation of specific polymorph and MC properties. Furthermore, the alkyl chain length had an obvious effect on the number of crystal polymorphs for **MDHP-C$_n$** and **TDHP-C$_n$**, that was, an increase in the alkyl chain length decreased the number of crystal polymorphs in trend. Single crystal analysis displayed that the difference in emissions of the polymorphs of the DHP derivatives mainly originated from their different intermolecular interactions and molecular packing patterns, whereas a subtle difference in the distances of the intermolecular interactions could also play a crucial role in the formation of the specific polymorphs. Different crystal polymorphs could be interconverted by a simple recrystallization process with a specific solvent, grinding, or fuming. These DHP derivatives had strong intermolecular interactions and/or π–π stacking interactions in the crystal structures, which made it difficult to transform them from a crystalline state to an amorphous

View Article Online
DOI: 10.1039/C7TC00362E

state upon grinding. The XRD and DSC experiments revealed that their MC properties could be ascribed to the phase transition between different crystalline states. The reason **TDHP-C$_8$**, **IDHP-C$_n$**, and **NDHP-C$_n$** did not have MC properties might be that they had only one type of crystal and thus could not realize the transformation from one crystalline state to another crystalline state. This work provides new information to for the development of organic fluorescent materials with MC and polymorphic properties.

Acknowledgements

This research work was supported by the National Natural Science Foundation of China (Grants 21572165, 21272176, and 21474048) and the Zhejiang Provincial Natural Science Foundation (Grant LY16B040005).

Notes and references

1 (a) J. Mei, Y. Hong, J. W. Y. Lam, A. J. Qin, Y. H. Tang and B. Z. Tang, *Adv. Mater.*, 2014, **26**, 5429–5479; (b) Z. G. Chi, X. Q. Zhang, B. J. Xu, X. Zhou, C. P. Ma, Y. Zhang, S. W. Liu and J. R. Xu, *Chem. Soc. Rev.*, 2012, **41**, 3878–3896; (c) X.Q. Zhang, Z. G. Chi, Y. Zhang, S. W. Liu and J. R. Xu, *J. Mater. Chem. C*, 2013, **1**, 3376–3390; (d) S. P. Anthony, *ChemPlusChem*, 2012, **77**, 518–531; (e) S. Varghese and S. Das, *J. Phys. Chem. Lett.*, 2011, **2**, 863–873; (f) Y. Sagara and T. Kato, *Nat. Chem.*, 2009, **1**, 605–610; (g) H. B. Sun, S. J. Liu, W. P. Lin, K. Y. Zhang, W. Lv, X. Huang, F. W. Huo, H. R. Yang, G. Jenkins, Q. Zhao and W. Huang, *Nat. Commun.*, 2014, **5**, 3601–3609; (h) Y. Sagara, S. Yamane, M. Mitani, C. Weder, and T. Kato, *Adv. Mater.*, 2016, **28**, 1073–1095.

2 (a) H. Y. Zhang, Z. L. Zhang, K. Q. Ye, J. Y. Zhang and Y. Wang, *Adv. Mater.*, 2006, **18**, 2369–2372; (b) Y. Zhao, H. Gao, Y. Fan, T. Zhou, Z. Su, Y. Liu, and Y. Wang, *Adv. Mater.*, 2009, **21**, 3165–3169; (c) K. Wang, H. Zhang, S. Chen, G. Yang, J. Zhang, W. Tian, Z. Su and Y. Wang, *Adv. Mater.*, 2014, **26**, 6168–6173; (d) Y. Dong, B. Xu, J. Zhang, X. Tan, L. Wang, J. Chen, H. Lv, S. Wen, B. Li, L. Ye, B. Zou, and W. Tian, *Angew. Chem. Int. Ed.*, 2012, **51**, 10782 –10785; (e) R. Davis, N. P. Rath and S. Das, *Chem. Commun.*, 2004, 74–75; (f) C. Li, X. Luo, W. Zhao, C. Li, Z. Liu, Z. Bo, Y. Dong, Y. Q. Dong and B. Z. Tang, *New J. Chem.*, 2013, **37**, 1696–1699; (g) R. H. Li, S. Xiao, Y. Li, Q. Lin, R. Zhang, J. Zhao, C. Yang, K. Zou, D. Li and T. Yi, *Chem. Sci.*, 2014, **5**, 3922–3928; (h) S. J. Yoon, J. W. Chung, J. Gierschner, K. S. Kim, M. G. Choi, D. Kim and S. Y. Park, *J. Am. Chem. Soc.*, 2010, **132**, 13675–13683; (i) K. Nagura, S. Saito, H. Yusa, H. Yamawaki, H. Fujihisa, H. Sato, Y. Shimoikeda and S. Yamaguchi, *J. Am. Chem. Soc.*, 2013, **135**, 10322–10325; (j) G. Q. Zhang, J. W. Lu, M. Sabat and C. L. Fraser, *J. Am. Chem. Soc.*, 2010, **132**, 2160–2162; (k) E. Sakuda, K. Tsuge, Y. Sasaki and N. Kitamura, *J. Phys. Chem. B*, 2005, **109**, 22326–22331; (l) X. Luo, W. Zhao, J. Shi, C. Li, Z. P. Liu, Z. S. Bo, Y. Q. Dong and B. Z. Tang, *J. Phys. Chem. C*, 2012, **116**, 21967–21972; (m) Y. Fan, Y. F. Zhao, L. Ye, B. Li, G. Yang and Y. Wang, *Cryst. Growth Des.*, 2009, **9**, 1421–1430; (n) X. G. Gu, J. J. Yao, G. X. Zhang, Y. L. Yan, C. Zhang, Q. Peng, Q. Liao, Y. Wu, Z. Z. Xu, Y. S. Zhao, H. B. Fu and D. Q. Zhang, *Adv. Funct. Mater.*, 2012, **22**, 4862–4872; (o) L. Chen, S. Y. Yin, M. Pan, K. Wu, H. P. Wang, Y. N. Fan and C. Y. Su, *J. Mater. Chem. C*, 2016, **4**, 6962–6966; (p) D. Yan and D. G. Evans, *Mater. Horiz.*, 2014, **1**, 46–57; (q) S. Ito, A. Hirose, M. Yamaguchi, K. Tanaka and Y. Chujo, *J. Mater. Chem. C*, 2016, **4**, 5564–5571; (r) S. Varughese, *J. Mater. Chem. C*, 2014, **2**, 3499–3516; (s) H. Wang, F. Chen, X. Jia, H. Liu, X. Ran, M. K. Ravva, F. Q. Bai, S. Qu, M. Li, H. X. Zhang and J. L. Brédas, *J. Mater. Chem. C*, 2015, **3**, 11681–11688; (t) M. J. Percino, M. Cerón, P. Ceballos, G. Soriano-Moro, O. Rodríguez, V. M. Chapela, M. E. Castro, J. Bonilla-Cruz and M. A. Siegler, *CrystEngComm*, 2016, **18**, 7554–7572; (u) S. J. Yoon and S. Y. Park, *J. Mater. Chem.*, 2011, **21**, 8338–8346; (v) Q. Qi, J. Zhang, B. Xu, B. Li, S. X. A. Zhang, and W. Tian, *J. Phys. Chem. C*, 2013, **117**, 24997−25003; (w) X. Du, F. Xu, M. S. Yuan, P. Xue, L. Zhao, D. E. Wang, W. Wang, Q. Tu, S. W. Chen and J. Wang, *J. Mater. Chem. C*, 2016, **4**, 8724−8730; (x) R. Tan, S. Wang, H. Lan, S. Xiao, *Curr. Org. Chem.*, 2017, **21**, 236−248.

3 (a) X. Cheng, H. Zhang, K. Ye, H. Zhang and Y. Wang, *J. Mater. Chem. C*, 2013, **1**, 7507–7512; (b) T. Seki, T. Ozaki, T. Okura, K. Asakura, A. Sakon, H. Uekusa and H. Ito, *Chem. Sci.*, 2015, **6**, 2187–2195; (c) P. S. Hariharan, D. Moon and S. P. Anthony, *J. Mater. Chem. C*, 2015, **3**, 8381–8388; (d) Y. Zhang, Q. Song, K. Wang, W. Mao, F. Cao, J. Sun, L. Zhan, Y. Lv, Y. Ma, B. Zou and C. Zhang, *J. Mater. Chem. C*, 2015, **3**, 3049–3054; (e) O. Toma, N. Mercier and C. Botta, *J. Mater. Chem. C*, 2016, **4**, 5940–5944; (f) C. Wang, B. Xu, M. Li, Z. Chi, Y. Xie, Q. Li and Z. Li, *Mater. Horiz.*, 2016, **3**, 220–225; (g) Y. X. Li, J. X. Qiu, J. L. Miao, Z. W. Zhang, X. F. Yang, and G. X. Sun, *J. Phys. Chem. C*, 2015, **119**, 18602–18610; (h) Z. Zhang, Z. Wu, J. Sun, B. Yao, P. Xue and R. Lu, *J. Mater. Chem. C*, 2015, **4**, 2854–2861; (i) R. Tan, Q. Lin, Y. Wen, S. Xiao, S. Wang, R. Zhang and T. Yi, *CrystEngComm*, 2015, **17**, 6674–6680; (j) Z. He, L. Zhang, J. Mei, T. Zhang, J. W. Y. Lam, Z. Shuai, Y. Q. Dong and B. Z. Tang, *Chem. Mater.*, 2015, **27**, 6601–6607; (k) B. Xu, J. He, Y. Mu, Q. Zhu, S. Wu, Y. Wang, Y. Zhang, C. Jin, C. Lo, Z. Chi, A. Lien, S. Liu and J. Xu, *Chem. Sci.*, 2015, **6**, 3236–3241; (l) X. Mei, G. Wen, J. Wang, H. Yao, Y. Zhao, Z. Lin and Q. Ling, *J. Mater. Chem. C*, 2015, **3**, 7267–7271; (m) Y. Qi, Y. Wang, Y. Yu, Z. Liu, Y. Zhang, G. Du and Y. Qi, *RSC Adv.*, 2016, **6**, 33755–33762; (n) C. Botta, S. Benedini, L. Carlucci, A. Forni, D. Marinotto, A. Nitti, D. Pasini, S. Righetto and E. Cariati, *J. Mater. Chem. C*, 2016, **4**, 2979–2989; (o) Yuanxiang Xu, Kai Wang, Yujian Zhang, Zengqi Xie, Bo Zou and Yuguang Ma, *J. Mater. Chem. C*, 2016, **4**, 1257–1262; (p) M. Jin, T. Seki and H. Ito, *Chem. Commun.*, 2016, **52**, 8083–8086; (q) B. Xu, Y. Mu, Z. Mao, Z. Xie, H. Wu, Y. Zhang, C. Jin, Z. Chi, S. Liu, J. Xu, Y. C. Wu, P. Y. Lu, A. Lien and M. R. Bryce, *Chem. Sci.*, 2016, **7**, 2201–2206; (r) P. Galer, R. C. Korošec , M. Vidmar, and B. Šket, *J. Am. Chem. Soc.* 2014, **136**, 7383–7394; (s) Y. Wang, G. Zhang, W. Zhang, X. Wang, Y. Wu, T. Liang, X. Hao, H. Fu, Y. Zhao and D. Zhang, *Small*, 2016, DOI: 10.1002/smll.201601516; (t) K. Sakurada, T. Seki and H. Ito, *CrystEngComm*, 2016, **18**, 7217–7220; (u) Meiqi Li, Qi Zhang, Jian-Rong Wang and Xuefeng Mei, *Chem. Commun.*, 2016, **52**, 11288–11291; (v) J. N. Zhang, H. Kang, N. Li, S. M. Zhou, H. M. Sun, S. W. Yin, N. Zhao and B. Z. Tang, *Chem. Sci.*, 2016, **7**, DOI: 10.1039/c6sc02875f.

4 Z. Guo, W. Zhu and H. Tian, *Chem. Commun.*, 2012, **48**, 6073–6084.

5 (a) C. Shi, Z. Guo, Y. Yan, S. Zhu, Y. Xie, Y. S. Zhao, W. Zhu, and H. Tian, *ACS Appl. Mater. Interfaces*, 2013, **5**, 192−198; (b) Z. Guo, A. Shao and W. H. Zhu, *J. Mater. Chem. C*, 2016, **4**, 2640–2646.

6 (a) H. Tong, M. Häussler, Y. Dong, Z. Li, B. Mi, H. S. Kwok and B. Z. Tang, *J. Chin. Chem. Soc.*, 2006, **53**, 243–246; (b) H. Tong, Y. Dong, M. Häussler, Y. Hong, J. Lam, H. Sung, I. D. Williams, H. S. Kwok and B. Z. Tang, *Chem. Phys. Lett.*, 2006, **428**, 326–330; (c) H. Tong, Y. Hong, Y. Dong, Y. Ren, M. Häussler, J. W. Y. Lam, K. S. Wong and B. Z. Tang, *J. Phys. Chem. B*, 2007, **111**, 2000–2007; (d) H. Li, Y. Guo, G. Li, H. Xiao, Y. Lei, X. Huang, J. Chen, H. Wu, J. Ding and Y. Cheng, *J. Phys. Chem. C*, 2015, **119**, 6737–6748.

View Article Online
DOI: 10.1039/C7TC00362E

7 (a) Y. Liu, Y. Lei, F. Li, J. Chen, M. Liu, X. Huang, W. Gao, H. Wu, J. Ding and Y. Cheng, *J. Mater. Chem. C*, 2016, **4**, 2862–2870; (b) Y. Lei, Y. Liu, Y. Guo, J. Chen, X. Huang, W. Gao, L. Qian, H. Wu, M. Liu and Y. Cheng, *J. Phys. Chem. C*, 2015, **119**, 23138–23148; (c) Y. Liu, Y. Lei, M. Liu, F. Li, H. Xiao, J. Chen, X. Huang, W. Gao, H. Wu and Y. Cheng. *J. Mater. Chem. C*, 2016, **4**, 5970–5980; (d) Y. Lei, D. Yang, H. Hua, C. Dai, L. Wang, M. Liu, X. Huang, Y. Guo, Y. Cheng and H. Wu, *Dyes Pigm.*, 2016, **133**, 261–272.
8 (a) K. C. Naeem, A. Subhakumari, S. Varughese and V. C. Nair, *J. Mater. Chem. C*, 2015, **3**, 10225–10231; (b) C. Niu, Y. You, L. Zhao, D. He, N. Na and J. Ouyang, *Chem. Eur. J.*, 2015, **21**, 13983–13990.
9 S. Xue, X. Qiu, Q. Sun and W. Yang, *J. Mater. Chem. C*, 2016, **4**, 1568–1578.
10 L. L. Woods. *J. Am. Chem. Soc.*, 1958, **80**, 1440−1442.
11 R. Boonsin, G. Chadeyron, J. P. Roblin, D. Boyer and R. Mahiou, *J. Mater. Chem. C*, 2015, **3**, 9580–9587.
12 G. Kwak, S. Wang, M.-S. Choi, H. Kim, K.-H. Choi, Y.-S. Han, Y. Hur and S.-H. Kim, *Dyes Pigm.*, 2008, **78**, 25–33.

View Article Online
DOI: 10.1039/C7TC00362E

Polymorphism and mechanochromism of *N*-alkylated 1,4-dihydropyridine derivatives containing different electron-withdrawing end groups

Yunxiang Lei, Yibin Zhou, Lebin Qian, Yuxiang Wang, Miaochang Liu, Xiaobo Huang, Ge Wu, Huayue Wu, Jinchang Ding and Yixiang Cheng

The electron-withdrawing groups of the *N*-alkylated 1,4-dihydropyridine derivatives are responsible for their reversible polymorphic and mechanochromic properties, and the length of the alkyl chain shows a significant impact on the number of their polymorphs.